(Online) ISSN 2744-1741
Original Research

Defense and Security Studies
Vol. 5, No. 2, 2024, pp.115-132
https://doi.org/10.37868/dss.v5.279

Estimation of internal ballistic parameters for the 107 mm rocket motor conceptual design

Ilma Subotić[1*]
[1] Center for Advanced Technologies Sarajevo, Bosnia and Herzegovina

*Corresponding author E-mail: ilma.subotic@outlook.com

Received: Nov. 3, 2024
Revised: Dec. 26, 2024
Accepted: Dec 27, 2024
Online: Dec. 31, 2024

Abstract

The demand for solid propellant rocket motors does not seem to fade, regardless of constant improvements in rocket technology. To make modifications that will result in improved design, it is crucial to use already existing motor models. Setting internal ballistic requirements and conducting calculations by following the design sequence, results in defining pressure- and thrust-time curves that are needed for rocket motor performance evaluation and providing a base for further external ballistic analysis. Calculation results are obtained by using the program SPPMEF, which is divided into modules for different parts of internal ballistic analysis using equations and shortens the time needed for theoretical integrations. NGR-176 is a type of double-base solid rocket propellant selected for the conceptual design of a 107 mm rocket motor. The selected propellant configuration is a star with adapted and optimized geometric variables and new structural materials have been assigned to the newly-sized nozzle and motor case through examining various parameters.

Keywords: internal ballistic, solid rocket propellant, rocket motor design

1. Introduction

Rocket projectiles represent a specific ammunition type, with a rocket motor included in their structure, the element that works by means of reactive force – thrust. Solid propellant rocket motors fall under the group of chemical rocket motors that represent a generator in which potential chemical force first converts into thermal energy of developed combustion gases, which further converts into the projectile's kinetic energy by gas expansion through the nozzle. The selection of solid propellant rocket motors is influenced by their simplicity, mobility, reliability, and efficiency, keeping the development and production costs at an acceptable level. Tactical projectiles with solid propellant rocket motors are usually used for firing at infantry, close strategic positions, military aircraft, and vessels [1, 2].

The conceptual design of the 107 mm rocket projectile starts with designing an effective solid propellant rocket motor by following the principles of rocket motor design, the technological potential of military production in Bosnia and Herzegovina, and the accessibility of materials on its market.

Calculations in internal ballistic (IB) of solid propellant rocket motors entail propellant composition and configuration selection that will ensure rocket motor performances that meet defined mission objectives, which include the formation and development of combustion gases after burning, such that the required thrust- and pressure-time curves are defined, which dictate values of dependent and independent IB parameters and initial projectile velocity, which further defines projectile's trajectory and range. To evaluate solid propellant rocket motor efficiency, parameters that need to be defined are: ballistic performances of the rocket motor (thrust force F, burning time t_b, total impulse I_{tot}), thrust coefficient C_F, combustion chamber pressure p_c and propellant properties [1].

1.1. Rocket motor structure, material and production technology selection

Four main components of a solid propellant rocket motor are: the motor case (chamber), propellant, nozzle, and igniter.

The motor case (chamber) is exposed to high temperatures and pressures during the propellant burning process, as well as high velocities of combustion gases during their expansion. That requires encasing the inner walls of the chamber with an isolating material that will be used as a binder between the propellant grain and walls. That could be an elastomer or a thermosetting plastic that is compatible with the selected propellant and which will provide a thermal shield and maximize erosion resistance from the hot gas flow [1].

The suggested production technology for the motor case is flow forming, which is based on the plastic deformation of a piece of metal on a mandrel by applying forces through rollers. This technology will provide: good dimension tolerance, geometrical precision during production, improvement of the material's mechanical properties, and lower the production cost [2].

The thickness of the rocket motor case is calculated by using the following equation, where the yield strength of steel C.4730 (AISI 4130) is known and equals R_p = 685 MPa [3]:

$$\delta_s = \frac{MEOP \cdot d \cdot k}{2R_p} = 2.7\ mm \tag{1}$$

where MEOP = 23.5 MPa is maximum expected operating pressure, d = 107 mm is caliber and k = 1.5 is security coefficient.

Motor case dimensions are important for limiting and, therefore, optimizing propellant grain dimensions. In this case, to achieve the desired performance of the rocket motor design, the grain length of L_{po} = 450 mm is accepted for the conceptual design, with the following values: L_{n1} = 21 mm – frontal motor case end where the warhead's bottom is attached, L_{n2} = 25 mm – rear motor case end where the nozzle is attached, L_d = 5 mm – propellant's distancer length.

Outer motor case diameter is known and equals D_v = 107 mm, whereas for the inner diameter for propellant design, inhibitor thickness (δ_{ip} = 1 mm for the outer grain surface and δ_{ip} = 2 mm for the front and rear end of the grain) and motor case wall thickness (δ_s = 2.7 mm) need to be taken into consideration and the calculated value equals D_u = 99.6 mm. Finally, the length/diameter ratio for the propellant grain is L_{po}/D_u = 4.52 and the free volume for grain placement is [3]:

$$V_a = \frac{{D_u}^2 \pi}{4} \cdot L_p = 0.0035061\ m^3 \tag{2}$$

The nozzle is the part of the rocket motor through which an intensive combustion gas expansion is happening, which means this part is thermally heavily loaded and exposed to erosion. The nozzle in this case is fixed and does not rotate during firing to direct developed thrust force, but it has 6 peripheral convergent-divergent (C-D) openings set at an angle of 22°, which allow the rocket to rotate and achieve gyroscopic (dynamic) stabilization. Considering

the nozzle's exposure to loads during the active phase of the motor and rocket's flight, the material selected for its production is steel C.4734 (AISI 4142), with a tensile strength of 1230-1430 MPa [2].

The propellant is the main source of energy for propulsion of solid propellant rocket motors and its configuration defines the burning process, initial mass flux of combustion gases, and initial thrust force. The selected propellant NGR-176 belongs to the homogenous solid rocket propellant group, usually referred to as double-base (DB) propellants. This kind of propellant is produced through extrusion, considering better mechanical properties they obtain, compared to propellants cast directly into the motor case, which have enhanced thermal effects due to chemical reactions between the propellant and casting agent [2, 4].

The composition of the introduced propellant with a density of ρ_p = 1590 kg/m^3 is given in Table 1 and the burning laws for three ambient temperatures (-30°C minimum, +20°C normal, and +50°C high) are given in Table 2. They are important for calculating burning velocity using Saint-Robert's law. Because of the plateau effect for pressures above 14 MPa, burning laws are different for the same ambient temperature, for the given value of pressure [3].

Table 1. Composition of propellant NGR-176 [3]

Nitrocellulose (NC)	55.24 (±1.5)
%N u NC	12
Nitroglycerin (NG)	33.84 (±1.0)
Diethyl phthalate (DEP)	2.96 (±0.4)
Ethyl centralite (EC)	2.96 (±0.4)
Lead stearate	2.00 (±0.5)
Calcium carbonate ($CaCO_3$)	2.00 (±0.3)
Grime	1.00 (±0.3)

Table 2. Burning laws for low (-30°C), normal (+20°C) and high (+50°C) ambient temperatures for NGR-176 [3]

Temperature	**a**	**n**	**Pressure value**
-30°C	0.005013	0.585523	≤ 14 MPa
	0.021131	0.038345	> 14 MPa
+20°C	0.006575	0.493339	≤ 14 MPa
	0.023985	0.005285	> 14 MPa
+50°C	0.005108	0.604111	≤ 14 MPa
	0.025013	0.002698	> 14 MPa

The configuration of the propellant for the 107 mm rocket motor, which is freestanding in the motor case, is star-shaped and defined by seven geometric variables (Figure 1): N – number of star points, w – web thickness, η – half-angle of the star ray, ξ – angle between the circle center that defines the root of star ray (tangential fillet) and the circle center that defines the top of star ray, r_1 – star root radius, r_2 – star point radius, Rp – grain radius. These dimensions are varied to satisfy grain optimization requirements. Parameters that define „star family" are: R_p, r_1, r_2, w and N, and the ones that ensure achieving the required volumetric fraction loading and degree of burning surface neutrality are angles ξ and η. The star-shaped configuration has a neutral burning character, provided by two dimensions that come from the interaction of star points that have regressive burning and cylinder that has progressive burning [1, 2, 5].

Despite the production process for the star-shaped configuration being complex, not being able to achieve a larger web fraction and lower chemical energy efficiency degree, this type of configuration shape is being selected because of its advantages [2]:

- inner motor case wall protection from hot combustion gases effect,

- achieving relatively constant burning surface area change with burned web thickness,
- smaller rocket motor slenderness.

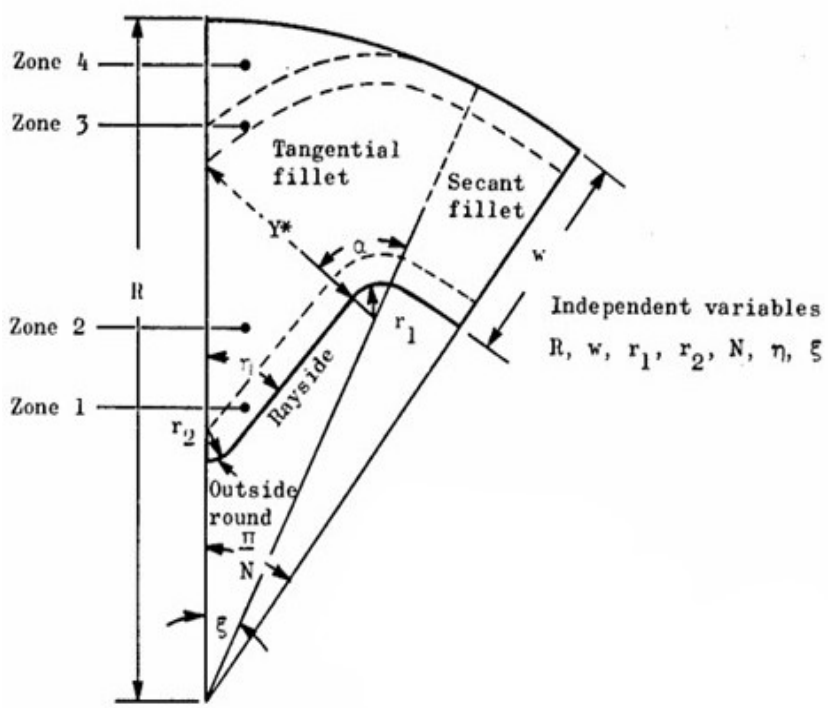

Figure 1. Geometric variables that define star-shaped configuration

The ignition system for the 107 mm rocket motor is pyrotechnic and consists of a composition that burns in such a manner that produces combustion gases that transfer directly onto the propellant grain and ignite it. The most important properties good ignition systems need to have are: high flame temperature (>≈ 3000 K), high burning rate (15-30 mm/s), and low ignition pressure. It has to meet the following requirements: security and reliability, ability to ignite propellant efficiently, minimal dimensions, steadfast pressure rise in the chamber, minimal time of grain surface ignition start, ability of long-term storage [1, 4, 6].

The selected ignition composition in this case is black powder consisting of: 74% potassium nitrate (KNO_3 – 2100 g/cm^3), 15% charcoal (C – 570 g/cm^3), and 11% sulfur (S – 1960 g/cm^3). It provides adiabatic flame of 2590 K. The impetus of black powder is λ = 254000 J/kg [4, 6].

The black powder is placed in a thin metal box placed on a threaded carrier that is put at the front end of the motor case, right below the warhead bottom. The wire that transfers the electric impulse used to start the ignition process is soldered at the place of contact on the inner surface of an aluminum lid that covers the nozzle before launching and it stretches from the lid, through the chamber, to the ignition composition carrier at the front end. Interior of the lid is isolated with a rubber insert to keep the heat transfer in control. The exit for formed ignition gases is positioned right above the front end surface of the propellant to start the combustion.

2. Research method

Estimating the internal ballistic parameters of the 107 mm rocket motor conceptual design by using adequate computer programs for calculations and CAD methods to create a 3-D model and 2D drawings is the base for the assessment of rocket motor performances. The steps required for a successful IB analysis are:

- defining mission objectives and constraints for the rocket in question,

- setting new ballistic requirements that will ensure achieving desired performances (pressure- and thrust-time curves),
- assessment of theoretic performances of the selected propellant, as well as energy properties of combustion gases,
- sizing of the new nozzle and rocket motor case,
- sizing and optimization of the propellant grain,
- sizing of the ignition system,
- assessment of IB parameters of the new rocket motor.

2.1. Program SPPMEF

SPPMEF (The Solid Propellant Rocket Motor Performance Prediction Computer Program) is a computer program made in the Department of Defense Technologies at Mechanical Engineering Faculty of University of Sarajevo, which uses defined ballistic requirements – average and minimal thrust, burning time, rocket mission requirements (MEOP, operational temperature range, launching height, envelope – motor case length and its inner diameter) and selected propellant type (defined composition, burning rate and temperature sensitivity). Entering the aforementioned requirements into the SPPMEF program provides the following results, calculated in four main modules of the program [7]:

- theoretical (ideal) performance prediction (TCPSP),
- assessment of losses in rocket motor and sizing of the nozzle (NOZZLE),
- sizing of propellant grain and burning surface area regression (GEOM),
- IB performance prediction (ROCKET).

2.2. SolidWorks CAD model

SolidWorks is the CAD program used to make a 3D model of the 107 mm rocket motor, as well as generate 2D drawings of newly sized and optimized parts. Materials from the SolidWorks library are used for every part of the rocket motor if the real material data is unavailable, otherwise, materials are defined by their mechanical properties. The following materials are considered for modeling rocket motor parts (Figure 2), with their mechanical properties shown in Table 3:

- steel AISI 4130 – motor case,
- steel AISI 4142 – nozzle,
- NGR-176 – propellant,
- phenol formaldehyde resin (PF plastic) – inhibitor,
- 1060 Al alloy – nozzle lid.

Table 3. Mechanical properties of materials applied in SolidWorks for rocket motor parts [8, 9, 10, 11, 12, 13]

	AISI 4130	**AISI 4142**	**1060 Al**	**PF**
Density [kg/m^3]	7850	7850	2700	1300
Tensile strength [MPa]	880-1080	1230-1430	90-110	35-62
Yield strength [MPa]	685	1030	65-85	28-50
Elastic modulus [GPa]	190-210	190-210	70-80	3.8
Poisson's ratio	0.27-0.3	0.27-0.3	0.33	0.33-0.36
Thermal conductivity [W/mK]	42.7	42.6	230	0.25

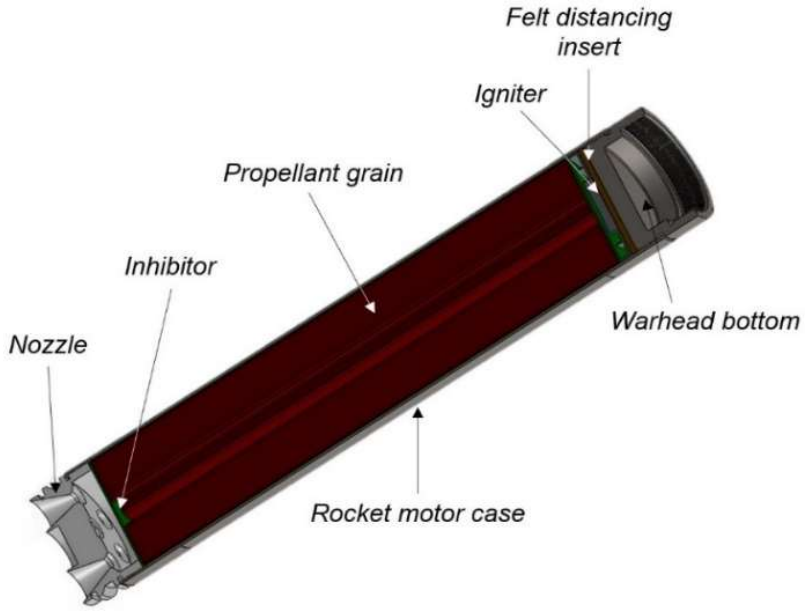

Figure 2. A 107 mm rocket motor assembly

3. Results and discussion

3.1. Defining ballistic requirements for the conceptual design of the rocket motor

The main step towards achieving the main objective is setting ballistic requirements, which include: total impulse, average thrust, and burning time. These parameters are important for defining pressure- and thrust-time curves, where the thrust-time curve serves for obtaining initial velocity after launching. Ballistic requirements for the 107 mm rocket motor are shown in Table 4:

Table 4. Ballistic requirements for the rocket motor [14]

Total impulse [Ns]	9180 Ns
Average thrust [N]	7061.54 N
Rocket motor burning time [s]	1.3 s

Web thickness can be approximated as a fourth of the inner diameter of the internal-burning propellant grain [1]:

$$w = \frac{D_u}{4} \approx 25\ mm = 0.025\ m \tag{3}$$

Propellant design usually requires reducing the web thickness by 2-3 mm, in this case, it is a 2.5 mm reduction, so the final web thickness is w = 0.0225 m.The burning rate is defined by coefficients a and n for a normal ambient temperature of 20°C and nominal pressure of 12.5 MPa, using Saint-Robert's law [15]:

$$r_b = a{p_{nom}}^n = 0.0229\ m/s \tag{4}$$

Web thickness is also defined as the average burning rate and rocket motor burning time ratio, so burning time can be determined by the following equation [4, 15]:

$$t_b = \frac{w}{r_b} = 0.98\ s \tag{5}$$

Average thrust force can be calculated using total impulse and burning time values [16]:

$$F = \frac{I_{tot}}{t_b} = 9367.35\ N \tag{6}$$

3.2. Thermochemical performances of propellant

Thermochemical properties of rocket propellants directly affect the selection and are used to define the energy properties of propellants, as well as IB parameters of a rocket motor. These parameters include: combustion products composition and their thermal capacity, average molecular mass, burning temperature and heat, etc. Theoretical analysis is an approximation of an actual combustion process inside a rocket motor chamber and its flow because more simple assumptions are needed. The analysis is carried out for two groups of calculations: combustion and expansion. Processes in the chamber are irreversible and non-isentropic. Rocket propellant efficiency depends on: a specific heat ratio γ, chamber temperature T_c, nozzle exit and chamber pressure ratio p_e/p_c, the molecular mass of combustion gases M [16, 17].

Module TCPSP in SPPMEF program is used to determine thermochemical properties for selected propellant (equilibrium and frozen expansion). It provides results in the form of: combustion gases' composition calculation under conditions of chemical equilibrium, their transport properties (dynamic viscosity and thermal conductivity coefficients and Prandtl number), and theoretical performances of a rocket motor with unknown surfaces. It is based on the following assumptions [18]:

- one-dimensional flow,
- the gas flow rate in the chamber is zero,
- combustion is complete and adiabatic,
- isentropic expansion in the nozzle,
- homogenous composition,
- combustion gases are behaving like an ideal gas,
- there are no differences in temperature and rate between the condensed and gas phases.

Theoretical performances of rocket motors are predicted for the following cases of expansion [18]:

- expansion up to a defined Mach number (a requirement for nozzle throat),
- expansion up to a defined pressure value at the exit cross-section of the nozzle,
- expansion up to three defined expansion ratios.

Calculations are based on values for combustion at a normal ambient temperature of +20°C. Transportation properties are shown in Table 5, and results of combustion parameters under conditions of equilibrium and frozen expansion are shown in Table 6.

Table 5. Transportation properties for equilibrium and frozen expansion

TRANSPORT PROPERTIES OF COMBUSTION GASES (EQUILIBRIUM)						
	Combustion chamber	**Critical section**	**Exit section**	**Exit section (Ae/At)**		
				6	**9**	**12**
Cp (J/gK)	1.8272	1.7804	5.3476	2.1367	2.6235	3.0229
Dv (Pas)10^5	7.268	6.7461	3.9989	4.3806	4.2177	4.1726
K (W/mK)	0.1896	0.1727	0.0879	0.0986	0.094	0.0927
Prandtl	0.7003	0.6955	2.4339	0.9492	1.1775	1.3607
TRANSPORT PROPERTIES OF COMBUSTION GASES (FROZEN)						
	Combustion chamber	**Critical section**	**Exit section**	**Exit section (Ae/At)**		
				6	**9**	**12**
Cp (J/gK)	1.7701	1.7417	1.47	1.529	1.5039	1.496
Dv (Pas)10^5	7.268	6.7335	3.6328	4.1632	3.9352	3.8645
K (W/mK)	0.1896	0.1719	0.0758	0.0906	0.0841	0.0821
Prandtl	0.6784	0.6822	0.7044	0.703	0.7038	0.704

Table 6. Combustion parameters for equilibrium and frozen expansion – NGR-176

EQUILIBIRUM EXPANSION						
	Combustion chamber	Critical section	Exit section	Exit section (Ae/At)		
				6	9	12
P (bar)	125.25	69.723	1.0132	2.5247	1.8127	1.635
T (K)	2351	2099.9	966.7	1102.2	1043.5	1027.5
Cp (J/gK)	1.8203	1.7713	4.5513	2.075	2.4805	2.8251
γs	1.2348	1.2416	1.1817	1.2242	1.2117	1.1984
S (J/gK)	9.627	9.627	9.627	9.627	9.627	9.627
H (J/g)	-2485.3	-2935.3	-5025.2	-4703.5	-4825.7	-4862.4
RH (g/m^3)	15494	9659	309.7	667.8	508.03	466
M (1/n)	24.182	24.187	24.568	24.243	24.313	24.345
MW (g/mol)	24.066	24.07	24.296	24.105	24.152	24.173
Vzv (m/s)	999	946.6	613.69	678.99	654.76	644.97
Mach	-	1	3.6726	3.102	3.3043	3.3806
c*(m/s)	-	1369.8	-	-	-	-
Ae/At	-	1	13.099	6	9	12
cf	-	1.24	1.6454	1.6161	1.6326	1.6365
Isp,v (Ns/kg)	-	1709.6	2399	2285.7	2328.4	2341.3
Isp,ad (Ns/kg)	-	948.7	2253.9	2106.3	2163.5	2180.4
Isp,na (Ns/kg)	-	1698.5	2253.9	2213.7	2236.2	2241.6
FROZEN EXPANSION						
	Combustion chamber	Critical section	Exit section	Exit section (Ae/At)		
				6	9	12
P (bar)	125.25	69.563	1.0132	2.353	1.6509	1.4757
T (K)	2351	2093	840.6	1021.6	942	917.9
Cp (J/gK)	1.7617	1.7335	1.4641	1.5225	1.4976	1.4898
γs	1.2425	1.2474	1.3069	1.2917	1.298	1.3
S (J/gK)	9.627	9.627	9.627	9.627	9.627	9.627
H (J/g)	-2485.3	-2936.3	-4967.6	-4697.2	-4817.4	-4853.4
RH (g/m^3)	15494	9666	350.6	669.8	509.66	467.56
M (1/n)	24.182	24.182	24.182	24.182	24.182	24.182
MW (g/mol)	24.066	24.066	24.066	24.066	24.066	24.066
Vzv (m/s)	1002.2	947.5	614.59	673.57	648.38	640.53
Mach	-	1	3.6254	3.1226	3.3308	3.3977
c*(m/s)	-	1367.5	-	-	-	-
Ae/At	-	1	11.725	6	9	12
cf	-	1.2405	1.6293	1.6076	1.6216	1.6246
Isp,v (Ns/kg)	-	1707.5	2357.8	2270.3	2309.7	2321.3
Isp,ad (Ns/kg)	-	949.7	2228.1	2103.3	2159.7	2176.3
Isp,na (Ns/kg)	-	1696.4	2228.1	2198.4	2217.6	2221.7

3.3. Nozzle sizing

The main objective of the nozzle design is an effective expansion of combustion gases from the chamber through the throat, creating sufficient thrust force. That means that nozzle sizing entices defining the throat area and

expansion ratio. Nozzle performances can be characterized with several parameters, from which the most notable ones are: nozzle (thrust force) efficiency coefficient η_{C_F}, mass rate coefficient , and thrust coefficient C_F [16].

With 6 C-D nozzle openings, the steps required for defining the throat area (expansion ratio) of the nozzle are [19]:

1. Calculating throat area with ideal thrust coefficient C_F^0 (maximum possible when ambient pressure is p_a = 0, maximum when exit pressure equals ambient pressure $p_e = p_a$) [2]:

$$A_t = \frac{F_{aver}}{C_F^0 \cdot p_c} \tag{6}$$

2. Calculating thrust force efficiency by inserting predicted losses during the gas expansion [2]:

$$\eta_{C_F} = 1 - 0.01 \cdot (\varepsilon_{DIV} + \varepsilon_{TP} + \varepsilon_{BL} + \varepsilon_{KIN} + \varepsilon_{EROS} + \varepsilon_{MULT}) \tag{7}$$

ε_{DIV} – flow divergence loss, ε_{TP} – two-phase flow loss, ε_{BL} – boundary layer loss, ε_{KIN} – kinetic loss, ε_{EROS} – nozzle erosion loss, ε_{MULT} – flow complexity loss.

3. Calculating real thrust coefficient $C_{F,r}$ [5]:

$$C_{F_{,r}} = \eta_{C_F} \cdot C_F^0 \tag{8}$$

4. Correction of throat area [6]:

$$A_t = \frac{F_{aver}}{C_{Fstv} \cdot p_c} \tag{9}$$

These steps are repeated until the convergence requirement is met for A_t and η_{C_F}, which is the difference between two A_t values being less than 1%.

The exit area and diameter of the nozzle are calculated using the following equations, respectively [3, 19]

$$A_e = A_t \cdot \varepsilon \tag{10}$$

$$D_e = \sqrt{\frac{A_e \cdot 4}{N}} \tag{11}$$

where N is the number of nozzle openings.

NOZZLE is the module of SPPMEF program used for nozzle sizing, and the following parameters are taken into consideration for calculations:

- thermochemical properties calculated in TCPSP module for equilibrium expansion,
- nozzle divergence half-angle α = 12°,
- expansion ratio ε = 9,
- number of nozzle openings N = 6,
- flow complexity loss ε_{MULT} = 1.65%.

Calculation results are shown in Table 7:

Table 5. Nozzle sizing and loss prediction using the NOZZLE module of SPPMEF program - NGR-176

	NGR-176
Theoretical specific impulse ε = 9, $I_{sp,th}$	2236.2 Ns/kg
Predicted specific impulse value, $I_{sp,p}$	1970.18 Ns/kg
Flow divergence loss, ε_{DIV}	1.093%
Two-phase flow loss, ε_{TP}	0.134%
Boundary layer loss, ε_{BL}	6.787%
Kinetic loss, ε_{KIN}	0.031%
Nozzle erosion loss, ε_{ER}	0.405%

Flow complexity loss, ε_{MULT}	1.65%
Thrust force efficiency coefficient, η_{C_F}	0.9
Thrust coefficient, C_F	1.47
Throat area, A_t	0.0005096 m^2
Throat diameter, D_t	10.4 mm
Exit area, A_e	0.0042398 m^2
Exit diameter, D_e	30 mm

3.4. Propellant selection and grain sizing

The main objective that propellant grain design needs to meet is achieving the required change of pressure in time, so the rocket mission can be carried out successfully. The conceptual design of propellant grain is highlighted by several features [7]:

- Consider propellant types that are available on the market and possible to make with technologies available in the industry.
- Configuration of propellant has to be defined in a way that ballistic requirements are met, keeping the structural integrity of the rocket motor at the same time.
- Approximately determine the structural integrity of the grain with the rise of chamber pressure during ignition.

Propellant grain selection is based on three segments: ballistic requirements assessment (according to rocket mission), configuration (geometry) selection, and analytical verification of the design. A specific occurrence in solid propellant rocket motors is the way the burning surface changes, so the relation between the burning area and the thickness of the burned web depends almost entirely on the initial grain shape [5].

The main factors considered in propellant grain configuration selection are [2]:

- free volume for grain placement V_a,
- L/D grain ratio,
- web thickness and grain radius ratio – web fraction:

$$w_f = \frac{w}{R_p} = \frac{2w}{D_u} = 0.452 \tag{12}$$

- pressure change type in the function of time (progressive, neutral or regressive burning),
- volumetric loading fraction V_l – determined by total and specific impulse requirements,
- critical loads – thermal cycles, pressure rise rate during ignition, acceleration, inner flow),
- production technology,
- production cost.

The selected star-shaped configuration for the 107 mm rocket motor allows a higher volumetric loading fraction, and has good burning surface neutrality, with a sliver value of 5-10% and web fraction (0.36-0.57 for V_l = 0.75-0.9 and 0.3-0.6 for V_l = 0.75-0.85) [16, 20].

GEOM is a module of SPPMEF consisting of two parts: propellant grain sizing and burning surface regression of the grain (change of burning area in time, in the function of current flame front position). Parameters required for propellant grain sizing are given in Table 8, calculated in the GEOM module [1].

Characteristic exhaust velocity c^* depends on combustion temperature T_c, gas constant R and specific heat ratio γ, and not significantly from the change of combustion pressure [19].

Table 6. Main parameters for propellant grain sizing, for the selected propellant type NGR-176

Characteristic exhaust velocity, c^*	1369.8 m/s
Combustion efficiency coefficient, η_{C^*}	0.98
Web fraction, w_f	0.452
Burning surface-to-throat ratio (Klemmung), K	251.33
Average burning area, $A_{b,aver}$	0.12808 m^2

Combustion efficiency coefficient η_{C^*} mainly depends on gas and metal particles retention time in the chamber and is also defined as the "completeness of metal additives burning in the rocket motor and a degree of chemical equilibrium between combustion gases" [2].

Burning surface-to-throat ratio (Klemmung), K has a value of 50-600 and is calculated using the following equation [2]:

$$K = \frac{A_b}{A_t} = \frac{{p_c}^{(1-n)}}{a \cdot \rho_p \cdot C^*} \tag{13}$$

3.5. Star configuration optimization

Requirements for the grain design can contradict each other, for example, minimum sliver, maximum V_l and quasi-neutral burning cannot be synchronized. That is why the optimization of a star-shaped grain configuration is done by modifying 7 geometric variables, based on the adopted volumetric loading fraction V_l, sliver σ (relative propellant loss), and degree of burning neutrality, all to meet rocket mission requirements [5].

OPTIM is a module in the SPPMEF program and is a part of the GEOM module in which optimization calculations are conducted. Optimization is based on the following settings [18]:

- All 7 variables that define star configuration are taken into consideration;
- Maximum and average burning perimeter ratio Γ is considered an independent parameter:

$$\Gamma = \frac{S_{max}}{S_{aver}} \tag{14}$$

For selected V_l, as well as the sliver, a minimum value of Γ_{min} is selected from the ones listed by the program to provide quasi-neutral burning for the given star geometry. Selected values (according to reference [2]) are:

- V_l = 0.85,
- Sliver, σ = 5-10%.

A tendency followed during the optimization process is to reduce r_1 and r_2 as much as possible, considering they influence burning surface neutrality and sliver value while meeting the requirement for Γ_{min}, but if the values are too small, that will cause a practical problem with the production of the grain, which can break during ignition or storage at low temperatures. On the contrary, if r_1 is increased, sliver also increases, and burning surface neutrality is disturbed. If r_2 is increased, without modifying the rest of the dimensions, V_l also reduces, but that does not affect sliver and burning surface neutrality much. If r_2 is reduced, the radius of the circle that is tangent to star points *r* is also reduced. The minimum value of *r* is achieved when the requirement η < π/N is met [1].

Grain length can be calculated using the following equation [3]:

$$L_p = \frac{A_b}{S_{aver}} \tag{15}$$

where average perimeter S_{aver} is defined as the arithmetic mean value of minimum and maximum perimeter sum.

Table 9 shows the results of OPTIM calculations, with values assigned to geometric variables that determine the final grain design, after which the grain length and mass are determined (Table 10).

Table 7. Values of star configuration variables after optimization calculations in OPTIM

Minimum value of maximum and average burning perimeter ratio, Γ_{min}	1.1557	**Star root radius, r_1**	3 mm
Number of star points, N	6	**Star point radius, r_2**	2 mm
Web fraction, w_f	0.451	**Star root angle, ξ**	27°
Web thickness, w	22.46 mm	**Star ray half-angle, η**	32.88°
Grain radius, R_p	49.8 mm	**Radius of the circle that is tangent to star points, r**	16.8 mm

Table 8. Initial propellant grain values after optimization for NGR-176

Average burning parameter, S_{aver}	0.285 m
Coefficient J	0.398
Initial burning area after optimization, $A_{b0,opt}$	0.11043 m^2
Initial port area after optimization, $A_{p0,opt}$	0.001281 m^2
Volumetric loading fraction, V_l	0.836
Grain length, L_p	450 mm
Grain mass, m_p	4.68 kg

Coefficient J characterizes gas flow conditions in rocket motor. If it's too high, it indicates the existence of a large drop in pressure inside gas ports and erosive burning, which is what usually happens after ignition. Inner gas flow is satisfied if the port-to-throat ratio is <0.5. Equation used to describe coefficient J is [18]:

$$J = \frac{A_t}{A_p} \tag{16}$$

3.6. Star propellant grain regression

Free propellant surface regression during the process of burning is perpendicular to grain surface and defines pressure- and thrust-time curve development. Current burning area of the propellant grain is defined with the equation [2]:

$$A_{bi} = S_i \cdot L_p \tag{17}$$

where S_i is the current burning perimeter.

For star configuration, there are 4 specific zones where burning is observed (Figure 3) [2, 5]:

1. Zone 1 – $0 \leq w_i \leq r_2$ – progressive burning for variable web burned $w_x < r_2$, where perimeter S_1 and port area A_{p1} are defined as:

$$\frac{S_1}{2N} = \left(R_p - w + w_i\right) \cdot \left(\frac{\pi}{N} - \xi\right) + (r_1 + w_i)\left(\frac{\pi}{2} - \eta + \xi\right) + \left(R_p - w - r_1\right)\frac{\sin\xi}{\sin\eta} - (r_1 + r_2)\tan\left(\frac{\pi}{2} - \eta\right) + (r_2 - w_i)\tan\left(\frac{\pi}{2} - \eta\right) \tag{18}$$

$$\frac{A_{p1}}{N} = \left(R_p - w + w_i\right)^2 \cdot \left(\frac{\pi}{N} - \xi\right) + (r_1 + w_i)^2 \left(\frac{\pi}{2} - \eta + \xi\right) + \left(R_p - w - r_1\right)\frac{\sin\xi}{\cos\eta}cos(\eta - \xi) - \left[\left(R_p - w - r_1\right)\frac{sin}{cos\,\eta} - (r_1 + w_i)\right]^2 tan\left(\frac{\pi}{2} - \xi\right) + (r_2 + w_i)^2\left[tan\left(\frac{\pi}{2} - \xi\right) - \left(\frac{\pi}{2} - \xi\right)\right] \quad (19)$$

where w_i represents the path of the flame front.

2. Zone 2 – $r_2 < w_i \leq$ Y* = $\left(R_p - w - r_1\right)\frac{sin}{cos\,\eta} - r_1$ – progressivity is determined by the derivative of the perimeter change function S = f (w_x), where S_2 and A_{p2} are defined as:

$$\frac{S_2}{2N} = \left(R_p - w + w_i\right) \cdot \left(\frac{\pi}{N} - \xi\right) + (r_1 + w_i)\left(\frac{\pi}{2} - \eta + \xi\right) + \left(R_p - w - r_1\right)\frac{\sin\xi}{\sin\eta} - (r_1 + + w_i)\,tan\left(\frac{\pi}{2} - \eta\right) \quad (20)$$

$$\frac{A_{p2}}{N} = \left(R_p - w + w_i\right)^2 \cdot \left(\frac{\pi}{N} - \xi\right) + (r_1 + w_i)^2\left(\frac{\pi}{2} - \eta + \xi\right) + \left(R_p - w - r_1\right)\frac{\sin\xi}{\cos\eta}cos(\eta - \xi) - \left[\left(R_p - w - r_1\right)\frac{\sin\xi}{\cos\eta} - (r_1 + w_i)^2\right]^2 tan\left(\frac{\pi}{2} - \xi\right) \quad (21)$$

3. Zone 3 – Y* < $w_i \leq w$ – burning has a tendency to be progressive, where S_3 and A_{p3} are defined as:

$$\frac{S_3}{2N} = \left(R_p - w + w_i\right) \cdot \left(\frac{\pi}{N} - \xi\right) + (r_1 + w_i)\left[\xi + arcsin\left(\frac{R_p - w - r_1}{r_1 + w_i}sin\,\xi\right)\right] \quad (22)$$

$$\frac{A_{p3}}{N} = \left(R_p - w + w_i\right)^2 \cdot \left(\frac{\pi}{N} - \xi\right) + (r_1 + w_i)^2\left[\xi + arcsin\left(\frac{R_p - w - r_1}{r_1 + w_i}sin\,\xi\right)\right] + \left(R_p - w + w_i\right)^2 sin\,\xi\left[cos\,\xi + \sqrt{\frac{(r_1 + w_i)^2}{\left(R_p - w + w_i\right)^2} - sin^2\xi}\right] \quad (23)$$

4. Zona 4 – w < $w_i \leq w_t$ – regressive burning, where S_4 and A_{p4} are defined as:

$$\frac{S_4}{2N} = (r_1 + w_i)\left[\xi + arcsin\left(\frac{R_p - w - r_1}{r_1 + w_i}sin\,\xi\right) - \pi + arccos\left(\frac{(r_1 + w_i)^2 + \left(R_p - w - r_1\right)^2 - R_p}{2(r_1 + w_i)\left(R_p - w + r_1\right)}\right)\right] \quad (24)$$

$$A_{pi}^{(i)} = \sum_{i=1}^{n_{p4}} A_{P4}^{(I-1)} + \frac{S_4^{(i)} + S_4^{(i-1)}}{2} \cdot \Delta w_i \quad (25)$$

Equation (25) shows the possibility of port area being defined numerically with the rectangle rule, where the initial area value is the one from the end of zone 3 and where Δw_i represents the integration step.

The maximum flame front path is labeled as w_t and defined as [1]:

$$w_t = \sqrt{\left[\left(R_p - w + r_1\right)sin\,\xi\right]^2 + \left[R_p - \left(R_p - w + r_1\right)cos\,\xi\right]^2} - r_1 \quad (26)$$

OPTIM calculations using equations (17) – (26) give results in the form of diagrams that show burning and port area change in function of web thickness for propellant NGR-176 (Figure 4, A), as well as the change of J and K coefficients in function of web thickness (Figure 4, B).

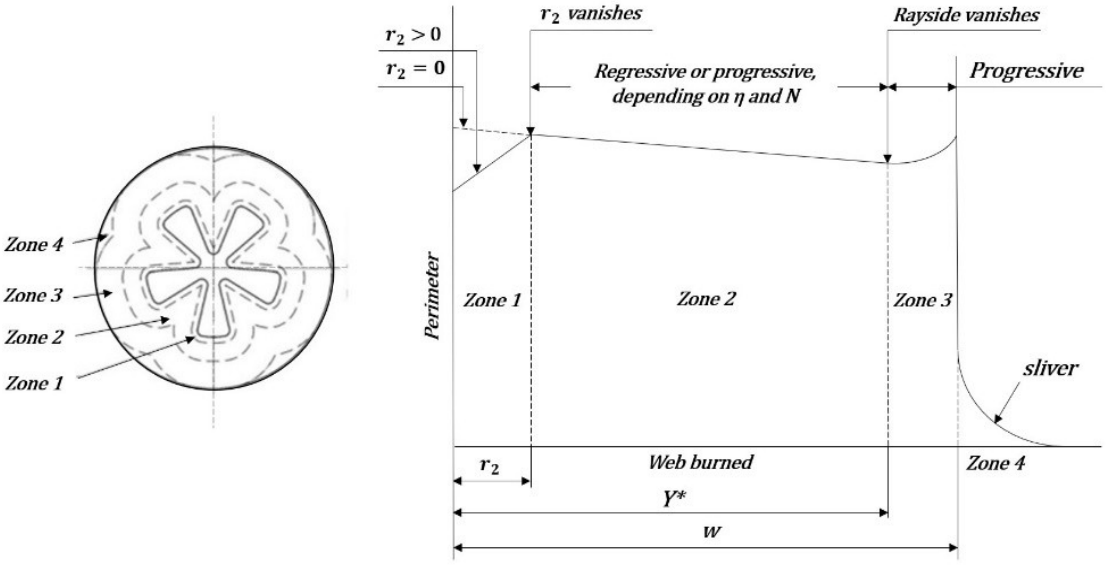

Figure 3. Star configuration burning zones [5]

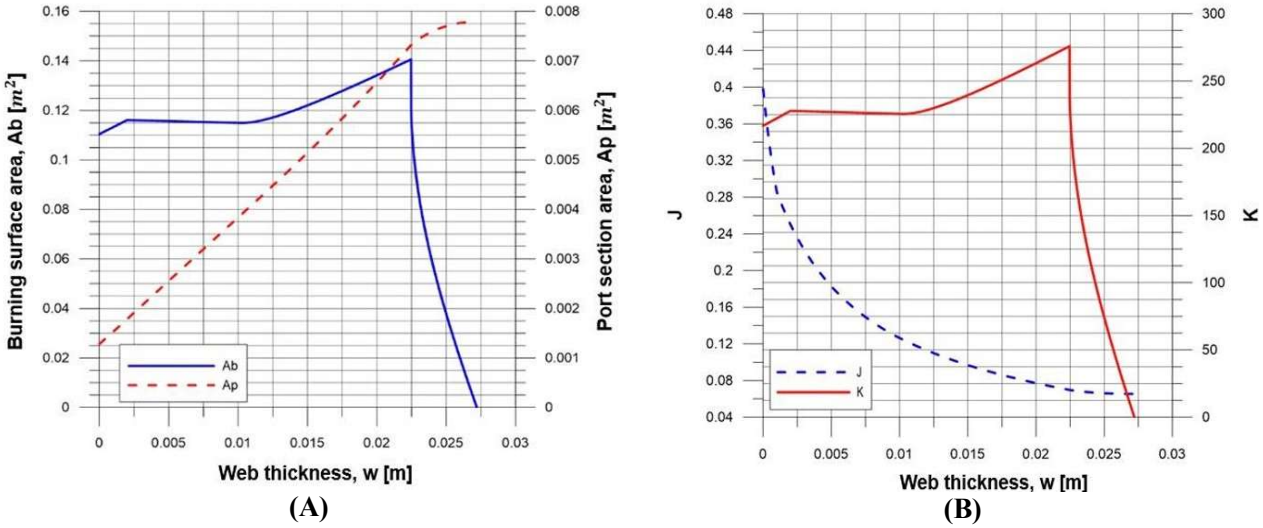

Figure 4. Diagrams of burning and port area change in function of web thickness (A) and J and K change in function of web thickness (B)

3.7. Internal ballistic parameters of the rocket motor for 107 mm, HE, XM24 ER

The final step in predicting IB parameters is concluding pressure-time (Figure 5) and thrust-time (Figure 6) curves for three accepted ambient temperatures, using calculation results obtained from SPPMEF program modules, which will give an insight into preliminary expectations for the rocket motor's behavior with selected propellant type and configuration, materials and production technologies, as well as the structural sizing done with the nozzle, motor case (chamber) and propellant grain.

ROCKET is the final SPPMEF module that provides prediction and display of results for the following parameters [18]: chamber pressure in function of time, nozzle exit pressure in function of time, thrust in function of time, burned propellant mass, nozzle throat area, current burning rate, thrust coefficient, total propellant mass, maximum and average value of thrust and combustion pressure, total impulse, specific impulse, pressure integral in function of time, burning time and total rocket motor action time. Calculation results are shown in Table 11.

Idealized prediction of IB performances of the rocket motor implies taking out the nozzle throat erosion effect, "hump" effect, and erosive burning, but they significantly affect performances, so it is necessary to take them into consideration. The following effects have been considered for the rocket motor:

- nozzle throat erosion with rate of 1 mm/s,
- erosive burning with coefficients: specific propellant heat c_s – 1450 J/kgK, burning surface temperature T_s – 650 K and empirical constant of β = 65,
- "hump" effect, according to factors shown in the reference [18].

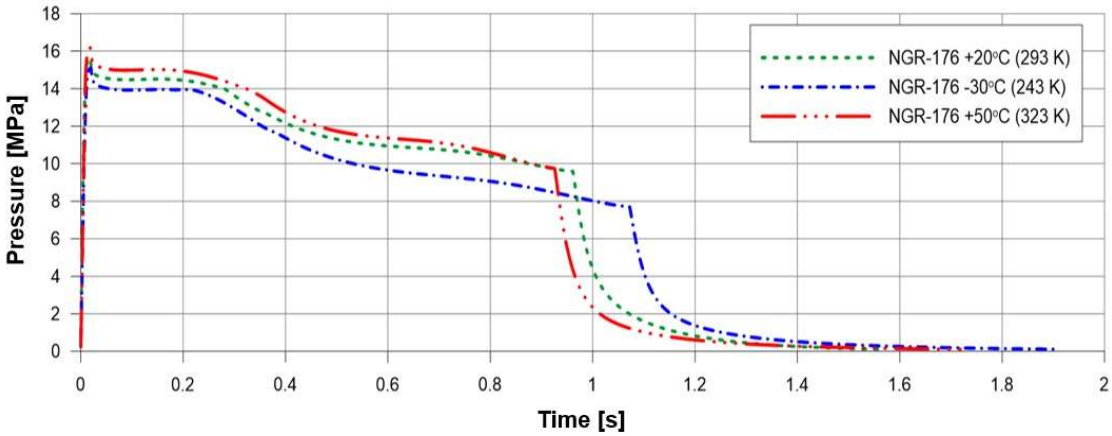

Figure 5. Pressure-time curve for normal (+20°C), low (-30°C) and high (+50°C) temperature, for optimized star-shaped propellant NGR-176

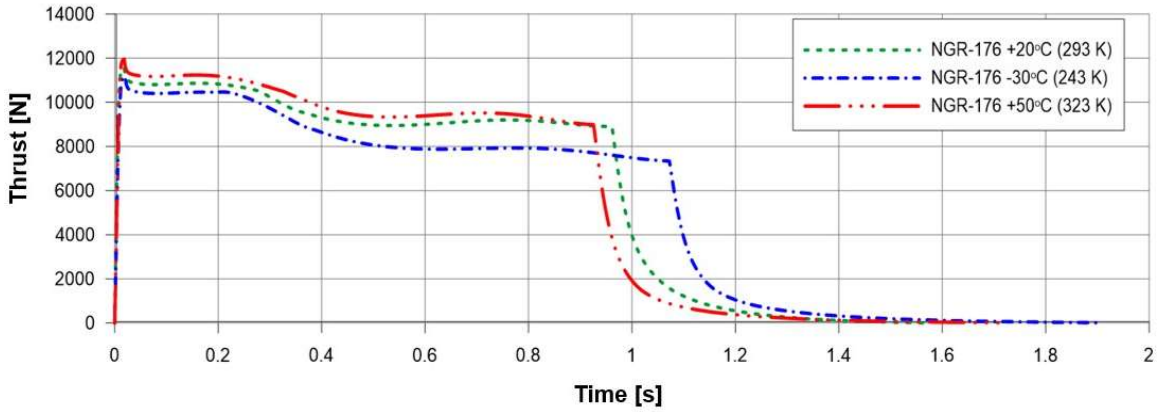

Figure 6. Thrust-time curve for normal (+20°C), low (-30°C) and high (+50°C) temperature, for optimized star-shaped propellant NGR-176

Table 9. IB parameters of the 107 mm rocket motor preliminary design

Ambient temperature, T	**Burning time, t_b [s]**	**Maximum pressure, p_{cmax} [MPa]**	**Maximum thrust, F_{cmax} [MPa]**	**Average thrust, F_{aver} [N]**	**Total impulse, I_{tot} [Ns]**
-30°C	1.07	15.31	11182.62	9131.57	9791.68
+20°C	0.96	15.87	11578.30	10252.77	9857.23
+50°C	0.93	16.41	11956.89	10591.02	9804.32

3.8. Sizing of the ignition system

The equation used to define the ignition mass of small- and average-sized rocket motors is derived from the ideal gas law for combustion gases at the end of ignition [3, 4]:

$$m_p = \frac{1}{1-\sigma} \cdot \frac{p_{cp} \cdot (V_a - V_p)}{\lambda} \tag{27}$$

Where p_{cp} is the initial chamber pressure after the ignition process, σ is the solid phase mass fraction of igniter combustion gases (20%) and V_p is propellant volume. Initial chamber pressure is calculated with the following equation [1]:

$$p_{cp} = (0.3\ do\ 0.4)p_{cnom} = 0.3 \cdot 12.525 = 3.76 \text{ MPa} \tag{28}$$

Ideal and real igniter densities are determined using the equation [1]:

$$\rho_{cp,ideal} = \frac{1}{0.01 \cdot \sum_{i=1}^{n} \frac{g_k}{\rho_k}} = \frac{1}{0.01 \cdot \left(\frac{g_{KNO3}}{\rho_{KNO3}} + \frac{g_C}{\rho_C} + \frac{g_S}{\rho_S}\right)} = 1492.56 \text{ kg/m}^3 \tag{29}$$

$$\rho_{cp} = l_f \cdot \rho_{cp,ideal} = 1119.42 \text{ kg/m}^3 \tag{30}$$

Where l_f = 0.75 is the real-ideal igniter density ratio and g_k is the solid phase fraction.

Using the calculated propellant mass m_p = 4.68 kg and known propellant density for NGR-176 ρ_p = 1590 kg/m^3, propellant volume totals:

$$V_p = \frac{m_p}{\rho_p} = 0.00294 \text{ kg/m}^3 \tag{31}$$

Finally, the igniter mass for the preliminary design of the 107 mm rocket motor is:

$$m_{pr} = 0.00907 \text{ kg} = 9.07 \text{ g} \tag{32}$$

4. Conclusions

According to calculations provided by the SPPMEF program, followed by structural modifications and design decisions, the selected propellant NGR-176 for the preliminary design of the 107 mm rocket motor provides an average thrust force of F_{aver} = 10252.77 N at +20°C, burning time of t_b = 0.96 s at +20°C and maximum chamber pressure of p_{cmax} = 16.41 MPa at +50°C (p_c = 15.87 MPa for +20°C), which meets set ballistic requirements. It is evident that the maximum pressure, predicted for the higher ambient temperature of +50°C stays under loading limits (MEOP), which is important for keeping the structural integrity and combustion process in control.

One effect that has not been considered for calculations is the radial acceleration effect on the overall display of thrust loss, which should be explored more, considering the type of stabilization this rocket has (gyroscopic). Materials and technologies described in this research are selected to adjust to production possibilities in Bosnia and Herzegovina. For further research, theoretical results should be verified through numerical simulations, as an introduction to real conceptual design analysis.

Declaration of competing interest

The author declares that she has no known financial or non-financial competing interests in any material discussed in this paper.

Funding information

No funding was received from any financial organization to conduct this research.

Acknowledgments

My deepest gratitude and admiration go to the entire personnel of the Defense Technologies Department of Mechanical Engineering Faculty, University of Sarajevo, as well as their external associates and academics for an immeasurable contribution to research in the domain of solid propellant rocket motors design and testing, which accounts for numerous research papers, proceedings and articles containing valuable experimental analysis, calculations, and program codes. These materials provided much-needed information for this paper, that stands as a base for further research.

References

[1] J. Terzic, Prediction the idealized internal ballistic features of the double base solid propellant rocket motors, Master thesis, Sarajevo: Mechanical Engineering Faculty, University of Sarajevo, 2002.

[2] M. Baskarad, Rocket motor structure influence on internal ballistic parameters of double-based propellants, Master thesis, Mostar: Mechanical Engineering, Computing and Electrical Engineering of University of Mostar, 2005.

[3] I. Vatric, Range improvement of the rocket projectile 122 mm, M-21OF, for multiple rocket launcher BM-21, Sarajevo: Mechanical Engineering Faculty of University of Sarajevo, 2014.

[4] D. Mishra, Fundamentals of rocket propulsion, Boca Raton, FL, USA: Taylor & Francis Group, LLC, 2017.

[5] Solid propellant grain design and internal ballistics, National Aeronautics and Space Administration, 1972.

[6] F. Williams, M. Barrere, N. Huang, Fundamental Aspects of Solid Propellant Rockets, England: Technivision Services Slough, 1989.

[7] J. Terzic, B. Zecevic, M. Baskarad, A. Catovic, S. Serdarevic-Kadic, "Prediction of internal ballistic parameters of solid propellant rocket motors," *Problems of Mechatronics: Armament, Aviation, Safety Engineering,* vol. 4, no. 6, pp. 7-26, 2011.

[8] B. Zecevic, J. Terzic, "The propulsion group's structure for the axially-symmetrical projectiles," in *III Međunarodni naučno-stručni skup "Tendencije u razvoju mašinskih konstrukcija i tehnologija"*, Zenica, 1996.

[9] "SAE AISI 4130 Chromoly steel, alloy material properties, chemical composition," World Material, [Online]. Available: https://www.theworldmaterial.com/sae-aisi-4130-chromoly-steel-alloy-material/. [Accessed 15 2 2025].

[10] "AISI 4142 alloy steel (UNS G41420)," AZO Materials, 17 9 2012. [Online]. Available: https://www.azom.com/article.aspx?ArticleID=6677. [Accessed 15 2 2025].

[11] "Aluminum alloy 1060 (UNS A91060)," Matmake, [Online]. Available: https://matmake.com/materials-data/aluminum-1060-properties.html. [Accessed 15 2 2025].

[12] "Phenol Formaldehyde (PF, Phenolic)," MakeItFrom.com, [Online]. Available: https://www.makeitfrom.com/material-properties/Phenol-Formaldehyde-PF-Phenolic/. [Accessed 15 2 2025].

[13] M. Ashby, *Material property data for engineering materials,* ANSYS - Education resources, 2021.

[14] *Tactical and technical characteristics of the standard "107" and "107-ER" rockets,* Beograd: EDePro.

[15] B. Zecevic, J. Terzic, "Estimating current burning rate in standard ballistic rocket motor," in *2. Medjunarodni skup, Revitalizacija i modernizacija proizvodnje RIM '99*, Bihac, 1999.

[16] G. Sutton, O. Biblarz, Rocket propulsion elements, Hoboken, NJ, USA: John Wiley & Sons Inc., 2010.

[17] F. Verhoek, Thermodynamics and rocket propulsion, Columbus, OH, USA: The Ohio State University, 1969.

[18] J. Terzic, Research influence of nozzles geometry on internal ballistic performance tactical rocket motors with double base propellant, PhD dissertation, Sarajevo: Mechanical Engineering Faculty, University of Sarajevo, 2012.

[19] B. Zecevic, Influence of variable field of high radial acceleration on solid propellant rocket motor internal ballistics, PhD dissertation, Sarajevo: Faculty of Mechanical Engineering, University of Sarajevo, 2012.

[20] B. Zeller, Solid propellant grain design, Paris: AGARD-LS-150, 1988.